International Journal of Power Electronics and Drive System (IJPEDS)
Vol. 11, No. 4, December 2020, pp. 1958~1965
ISSN: 2088-8694, DOI: 10.11591/ijpeds.v11.i4.pp1958-1965

An improved method for efficient controlling of the dynamic voltage restorer to enhance the power quality in the distribution system

Ali Basim Mohammed[1], Mohd Aifaa Mohd Ariff[2], Sofia Najwa Ramli[3]
[1] Faculty of Electrical and Electronic Engineering, University Tun Hussein Onn Malaysia, Malaysia.
[2,3] Faculty of Computer Science and Information Technology, Universiti Tun Hussein Onn Malaysia, Malaysia.

Article Info

Article history:

Received Dec 11, 2019
Revised Feb 12, 2020
Accepted Jum 3, 2020

Keywords:

Dynamic voltage restorer
PID controller
Power quality
Sliding mode controller
Voltage sag/swell

ABSTRACT

This paper represents a low complexity of the DVR controller by using a robust differentiator named as approximate classical sliding mode differentiator (ACSMD) to overcome the drawback of the linear differentiator. Additionally, utilize a nonlinear sliding variable named arctan function (sigmoid function) in order to keep the magnitude of the load voltage approximately 1pu, the THD at the standard level, improve the robustness property and maintain the steady-state error within a small bound. The most important issues of the power system network are power quality, the major problems of power quality are voltage sag/swell and harmonics which cause tripping or malfunctioning of the equipment. This paper gives an economic and effective solution by utilizing the dynamic voltage restorer to protect the sensitive loads from the disturbances that happened in the system such as voltage sag/swell and harmonics. The proposed system of the DVR is investigated by utilizing MATLAB/Simulink to enhance the disturbances when it occurs in a distribution system. The presents DVR model is evaluated by utilizing some of the popular voltage sag indices.

Corresponding Author:

Mohd Aifaa Mohd Ariff
Faculty of Electrical and Electronic Engineering,
University Tun Hussein Onn Malaysia (UTHM),
86400, Malaysia.
Email: aifaa@uthm.edu.my

1. INTRODUCTION

In a distribution system, power quality has attracted researchers and operators' attention due to the increment of the power electronic equipment and the non-linear load utilization [1]. The power quality issues such as voltage sag and voltage swell affect the performance of the consumer sensitive equipment. Thus, it is necessary to improve the quality of the power delivered to the user. In practice, there are various methods reported to improve the power quality in the distribution network. One of the solutions is the utilization of the dynamic voltage restorer (DVR) to mitigate the harmonics and compensate for the voltage sag and swell during power system operation [2-4]. The DVR is utilized by controlling the voltage source connected in series between the loads and the grid. It is used to regulate any disturbances that affect sensitive loads [5-7]. In the literature, there are several types of DVR controllers reported, such as feed-forward and feedback [8], fuzzy and adaptive proportional-integral-fuzzy controllers [9].

Sliding mode control (SMC) is a control method used with the DVR to regulate the voltage supplied to the three-phase load. SMC is preferred in various nonlinear control applications due to its fast response, easier to implement, and robust with the variation of the system parameters. In the literature, the SMC for the

DVR application is reported in [10]. The method uses 12-switch, 3-phase voltage source converter to provide the required compensation following a voltage disturbance. Next, a multilevel SMC combines a three-phase inverter and three single-phase inverters to inject the voltage compensation to the system [11]. The power converters are controlled by the SMC. On the other hand, the SMC controls a single-phase DVR by tuning the parameters of the controller [12]. In [13], the SMC is utilized with the DVR to address the issue of voltage sag in the system, specifically. The particle swarm optimization technique is utilized in [14] to estimate the optimum parameters of the SMC to mitigate the THD of the voltage. The SMC utilized in this report is based on the synchronous reference frame to obtain the DVR reference voltage. The majority of the SMC reported in the literature is based on a variant of a linear sliding variable with a linear differentiator to obtain the derivative of the error function. Although it has shown satisfactory performance in the various report, its application is limited to the presence of noise the measured input signal, which is inevitable in practice.

This paper presents a robust SMC technique for DVR to address the limitation of the linear controller. The method is based on the approximate classical sliding mode differentiator (ACSMD) with the nonlinear sliding variable (NSV). In this paper, the sigmoid function is used to define the appropriate control response based on the input to mitigate the voltage disturbance that occurred in the system. The proposed method is robust against the presence of noise in the measured input signal. Consequently, this allows the DVR to maintain the voltage magnitude at the constant value, minimize the steady-state error bound, and reduce the total harmonic distortion of the system. Following this introductory section, the proposed methodology of the ACSMD with NSV is discussed in Section 2. This section elaborates on the ACSMD in detail, the selection of the NSV method, the description of the test system model, and the performance indicator utilized in this study. Next, the proposed methodology is applied, and the results are analyzed in Section 3. Finally, Section 4 concludes the work presented in this paper.

2. METHODOLOGY

This section discusses the methodology proposed in this study. The section starts with the elaboration of the ACSMD technique, followed by the selection of the NSV approach. Then, the test system model and the performance evaluation measurement are discussed.

2.1 Approximate classical sliding mode differentiator (ACSMD)

The ASCMD works by estimating the error signal e as in (1).

$$e = x + \sigma \tag{1}$$

From the equation, e is the error in the input signal, x is the observer dynamic, σ is the observer sliding variable, respectively. The observer dynamic x is obtained form its derivative function formulated in (2). In (2), the gain k and f are the sliding mode differentiator gain, respectively. The gain k and f are selected to force σ goes to zero as $k > |\dot{e}|$. Consequently, let the estimation of $\dot{e}$ become the output of the following low pass filter (LPF) as in (3).

$$\dot{x} = -\frac{2k}{\pi} * \tan^{-1}(f\sigma) \tag{2}$$

$$\tau\dot{v} + v = \frac{2k}{\pi} * \tan^{-1}(f\sigma) \tag{3}$$

From (3), τ is a time constant of the low pass filter (LPF), and v is the LPF output, respectively. Eventually, the derivative of the LPF output is represented as in (4). The derivative of the LPF output is the output of the ACSMD method [15].

$$\dot{v} = \frac{1}{\tau}(-v + \frac{2k}{\pi} * \tan^{-1}(f\sigma)) \tag{4}$$

The selection of the time constant of the LPF and the gain f are very critical to the performance of the ACSMD technique. In this study, these parameters are set based on the study reported in [15]. These parameters should be selected such that (4) is minimized. Therefore, these two parameters are set such that $\frac{2}{\tau f}$ is as small as possible. In this study, τ is set to 0.01, and f is set to 100, respectively. In addition, τ should be set small enough to eliminate the high-frequency term in the input error signal.

2.2 Sliding variable approach

2.2.1. Linear PID sliding variable

The proportional, integral, and derivative (PID) controller has been utilized in the various control application in practice. Over 90% of the industrial processes utilize PID in their daily operation [16, 17] due to its robustness, ease of maintenance, and simplicity [18, 19]. The PID controller consists of proportional, integral, and derivative gains that scale the value of error ε between the input and output of the controller. In the sliding variable technique, the sliding variable S_{linear} based on the PID controller is represented using (5).

$$S_{error} = K_{\mathrm{P}}\varepsilon(t) + K_{\mathrm{I}}\int_0^t \varepsilon(t)dt + K_{\mathrm{D}}\frac{d\varepsilon(t)}{dt} \quad (5)$$

In (5), K_{P}, K_{I}, and K_{D} represent the proportional, integral, and derivative gains, respectively.

2.2.2. Nonlinear sliding variable

In the following items, the nonlinear sliding variables are proposed. The sliding variable will contain a nonlinear term which it functions to the error signal.

$$S(e) = \dot{e} + \lambda f(e) \quad (6)$$

Where S(e) is the linear sliding variable, $\dot{e}$ is the linear derivative of the error, λ is the sliding variable parameters, $f(\mathrm{e})$ is a linear function of e. The sliding variable becomes linear. In the actual situation, S(e) is not equal to zero in the sliding mode. Instead, S(e) will be highly oscillated and bounded signals. In the following subsections, the nonlinear sliding variable is suggested where $f(\mathrm{e})$ is a nonlinear function of the e. In addition, the robustness will be tested. This will show the superiority of the nonlinear against the linear sliding variable. Equation (7) represents a mathematical function that has a sigmoid curve or S-shaped characteristic of the curve. The logistic function shown below is the standard below choice for a sigmoid function [20].

$$S(x) = \frac{1}{1+e^{-x}} = \frac{e^x}{1+e^x} \quad (7)$$

Where $S(x)$ is the sliding variable of the function x, from the information above, the sigmoid function is monotonic and have the first derivative as bell-shaped, it is constrained by a pair of horizontal asymptotes as x→ ± ∞. It is convex for values is less than 0, and it is concave for values more than 0. For these specifications, sigmoid function and its affine compositions can possess multiple optima.

$$f(x) = arctanx \quad (8)$$

In the present work, the arctan function is used in the construction of the sliding variable. Accordingly, the sliding variable becomes;

$$S(\mathrm{e}) = \dot{e} + \lambda * \tan^{-1}(\alpha * e) \quad (9)$$

In this equation. S(e) is the sliding variable, α, and λ are the sliding variable parameters, and e is the input error signal. As in the previous two cases of the sliding variable, the ultimate bound on the error e can be estimated via Lyapunov function as follows;

$$\dot{\mathrm{V}} = \{-\lambda * \tan^{-1}(\alpha * \mathrm{e}) + \mathrm{S}\} * \mathrm{sign}(\mathrm{e}) \leq -\lambda * \tan^{-1}(\alpha * |\mathrm{e}|) + \rho \quad (10)$$

Where $\dot{\mathrm{V}}$ is the derivative of Lyapunov function, sign(e) is the signal function, and ρ is a positive constant, the ultimate bound on the error $e(t)$ is determined as;

$$|\mathrm{e(t)}| \geq \frac{1}{\alpha}\tan\left(\frac{\rho}{\lambda}\right), \text{as t} \to \infty \quad (11)$$

From the above inequality, the ultimate bound on e can be adjusted to a suitable value via a proper selection of the design parameters λ and α.

2.3 Voltage sag indices for performance evaluation

In order to evaluate the performance of the proposed method, several voltage sag indices that are typically used to determine the effectiveness of the method to improve power quality are considered in this study [21, 22]. They are listed in Table 1.

Table 1. Voltage sag indices for performance evaluation

Voltage sag indices	Formula	Parameters definition
Detroit Edison Sag Score (SS)	$SS = 1 - \frac{V_A + V_B + V_C}{3}$	$\boldsymbol{V_A}$, $\boldsymbol{V_B}$, $\boldsymbol{V_C}$ are voltage for Phase A, B, and C, respectively
Voltage Sag Lost Energy Index (VSLEI)	$VSLEI = T\left[1 - \frac{V(t)}{V_{nom}}\right]^{3.14}$	$\boldsymbol{V}_{nom}$ is the nominal voltage, V the phase voltage, and T is the time during the voltage sag.
Voltage Sag Energy ($\boldsymbol{E_{VS}}$)	$E_{VS} = \int_0^T \left[1 - \left(\frac{V(t)}{V_{nom}}\right)^2\right] dt$	

3. APPLICATIONS, RESULTS, AND DISCUSSIONS

3.1. The modeling of system and simulation

The proposed system of the DVR is investigated by using MATLAB/Simulink to simulate the disturbances when it occurs in a distribution system. The disturbances considered in this study are balanced sag, unbalanced sag, balanced swell, and unbalanced swell. The parameters of the test system model are obtained in [23]. Figure 1 represents the system under study. The system consists of an AC source that feeds the two feeders through a three-winding transformer. Each feeder connected to a winding transformer to supply the required power to different types of loads. The DVR connected in series with the second feeders to mitigate the voltage disturbance occurred in the system by injecting a required voltage.

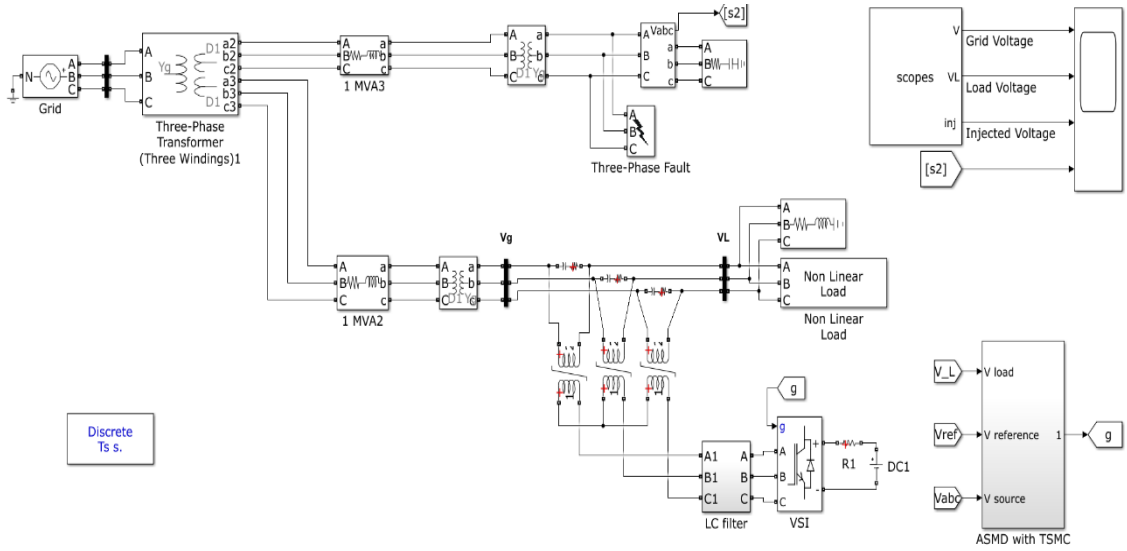

Figure 1. MATLAB/Simulink of the system under study

3.1.1. Case 1: Balanced three-phase voltage sag

A balanced voltage sag is applied to the system by overloading the load at t=0.1s until t=0.15s. Then, the induction motor in the system is overloaded at t=0.185s until t=0.2s. Consequently, the voltage amplitude is reduced in all three phases, as depicted in Figure 2(a). In the figure, the voltage is reduced from the nominal voltage to 0.7096 pu and 0.612 pu for the two operating situations, respectively. Consequently, the DVR senses this disturbance and injects a required voltage magnitude as shown in Figure 2(b). As a result, the voltage amplitude at the load side increases, as shown in Figure 2(c). Following the compensation, the voltage increases to 0.999pu, 0.9992pu, and 0.9992pu in Phase A, B, and C, respectively. In addition, the total harmonic distortion (THD) at the load voltage before compensation is 8.79. The THD improves to 1.41 following the compensation of the proposed DVR technique. The result discusses in this study corroborated with the result reported in [24].

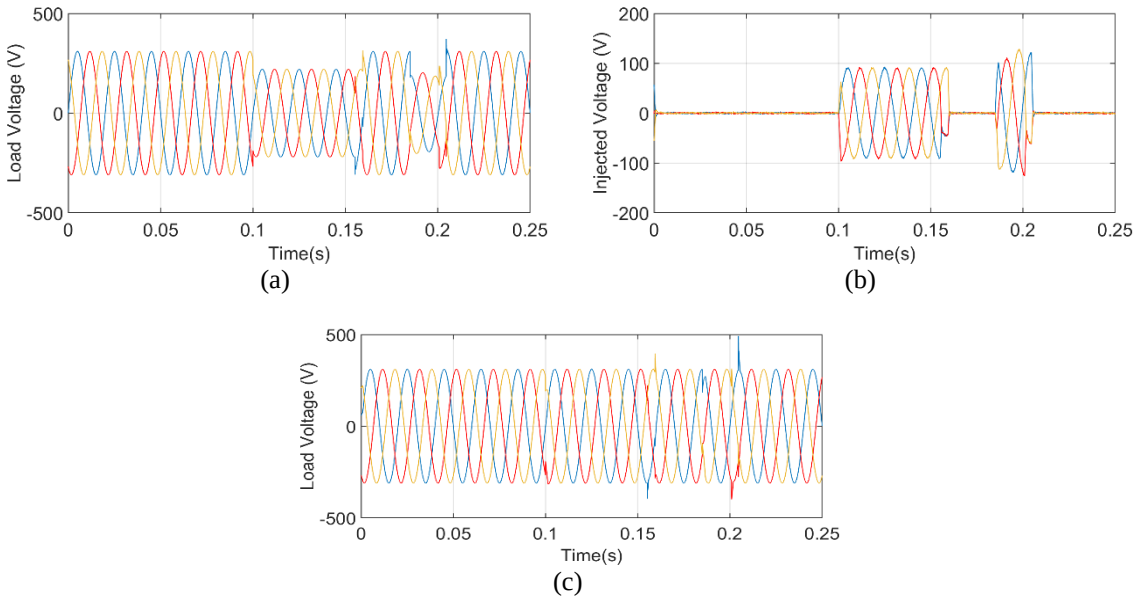

Figure 2. Simulation results for balanced voltage sag based DVR: (a) the uncompensated load voltage, (b) the voltage injects by DVR, (c) the compensated load voltage.

3.1.2. Case 2: Unbalanced voltage sag

In this study, the load is overloaded at t=0.2s until t=0.3s. Only phase C is applied to simulate the unbalanced voltage sag condition. Following this disturbance, the voltage amplitude is reduced to 0.4996pu, 0.8992pu, and 0.9007pu in Phase A, B, and C, respectively, as shown in Figure 3 (a). Then, the DVR detects the voltage sag and rapidly inject a proper magnitude to regulate the voltage at the load side as in Figure 3 (b). Consequently, the voltage amplitude at all three phases is restored to 0.9993pu, 0.9993pu, 1.0000pu in Phase A, B, and C, respectively. Figure 3(c) shows the compensated voltage of this case study. Additionally, the THD at the load improves from 15.78, before the compensation, to 1.71 after the compensation using the proposed DVR.

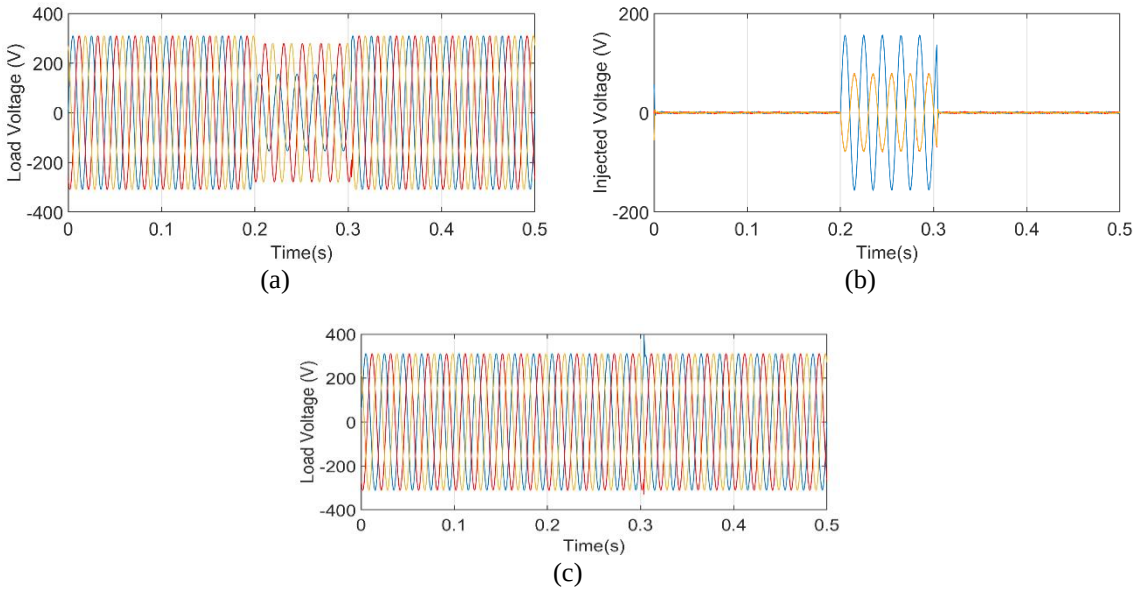

Figure 3. Simulation results for unbalanced voltage sag based DVR: (a) the uncompensated load voltage, (b) the voltage injected by DVR, (c) the compensated load voltage.

3.1.3. Case 3: Balance three-phase voltage swell

In this case study, the load is suddenly turned-off to simulate the voltage swell disturbance in the system. The voltage swell occurs at t=0.1s until t=0.2s. Figure 4(a) shows the voltage swell that occurred in the system. The figure shows that the voltage increases from the nominal voltage to 1.398pu in all phases. Following this voltage swelling, the DVR sense this difference and inject a required voltage magnitude. Figure 4(b) shows the phase voltage injected by the proposed DVR to compensate for the load voltage difference. Figure 4(c) represents the voltage amplitude at the load side after compensation. The result indicates the voltage at all phases improves to 0.9998pu. Moreover, the THD at the load bus before the compensation is 10.85. The compensation by the proposed DVR improves the THD to 0.87.

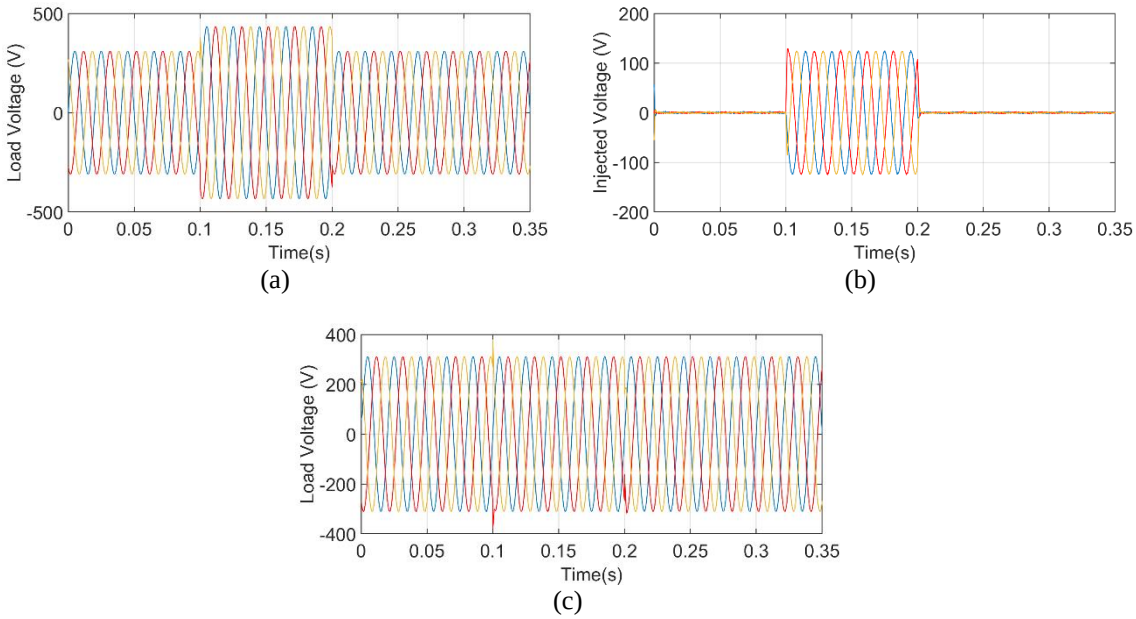

Figure 4. Simulation results for balance voltage swell based DVR: (a) the uncompensated load voltage, (b) the voltage injects by DVR, (c) the compensate load voltage.

3.1.4. Case 4: Unbalanced voltage swell

This case considers an unbalanced voltage swell occurred at t=0.2s until t=0.3s. In this operating situation, the voltage at Phase A, B, and C increases to 1.408pu, 1.146pu, and 1.124pu, respectively. This result is observed in Figure 5(a). Subsequently, the DVR detects the disturbance and injects a required voltage magnitude to mitigate the voltage disturbance, as shown in Figure 5(b). Figure 5(c) shows the load voltage following the compensation using the proposed DVR. In the figure, the load voltage in Phase A, B, and C increases to 0.9998pu, 1.0000pu, 0.9994pu, respectively. Plus, the THD at the load bus improves from 11.10 to 0.85 after the compensation.

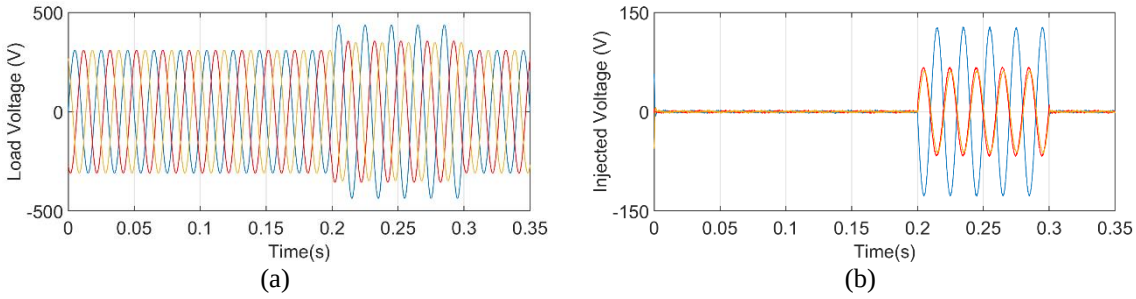

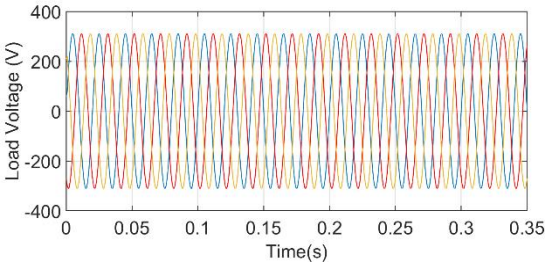

(c)

Figure 5. Simulation results for unbalanced voltage swell based DVR: (a) the uncompensated load voltage, (b) the voltage injected by DVR, (c) the compensated load voltage.

3.2. Performance evaluation

Table 2 summarizes the performance of the proposed work in mitigating the voltage disturbance. The performance is evaluated by utilizing the indices named SS,$VSLEI$ and E_{VS}. The results show that the ACSMD with the Arctan method improves the voltage quality in terms of SS,$VSLEI$ and E_{VS}. This improvement implies that the ACSMD with the Arctan method is able to mitigate the system voltage in the presence of the balanced and the unbalanced voltage sag.

Table 2. Voltage sag indices for ACSMD with arctan

Voltage sag indices	VSLEI (pu)		E_{VS} (pu)		*SS* (pu)	
Fault type	Before	After	Before	After	Before	After
Balance voltage sag	3.0896	3.7876×10^{-8}	12.6498	1.1400×10^{-4}	0.2904	8.6667×10^{-4}
Unbalanced voltage sag	11.5177	2.4811×10^{-8}	27.0421	9.8000×10^{-5}	0.2335	4.6667×10^{-4}

Table 3 tabulates the performance comparison of the proposed method with the method reported in [23]. The performance is measured using the integral time absolute error (ITAE). The disturbances considered in this study are similar to the cases discussed in the previous sections. From the table, the proposed DVR method outperforms the method reported in [23] in all cases. The result implies that the proposed work minimizes the error in compensating the voltage as compared to the method in [23].

Table 3. Illustrate a comparison between the results in [23] with the proposed work ACSMD with arctan

Operating conditions	ITAE(DC) [23]	ITAE (DC)
Balance voltage sag	1.623	0.1119
Unbalance voltage sag	1.487	0.1752
Balance voltage swell	1.668	0.1238
Unbalance voltage swell	1.689	0.07127

4. CONCLUSION

In conclusion, this paper reports a DVR controller method using the ACSMD with the Arctan method. The results show that the proposed method is able to compensate for the voltage in the test system model under the balanced voltage sag, unbalanced voltage sag, balanced voltage swell, and unbalanced voltage swell. Following the compensation, the THD at the load bus is also improved. The comparison analysis of the method with the method reported in the literature has been discussed in this paper. The result indicates that the proposed method shows a better performance in terms of ITAE as compared to the method reported in the literature. This implies that the ACSMD with the Arctan method is able to compensate the voltage under various voltage disturbances better as compared to the method discussed in this paper.

ACKNOWLEDGEMENTS

The authors would like to thank Universiti Tun Hussein Onn Malaysia (UTHM), Johor, and Ministry of Education (MOE) Malaysia for the award of the grant that enabled this research under grant No. H208.

REFERENCES

[1] A. B. Mohammed, M. A. M. Ariff, and S. N. Ramli, "Power quality improvement using dynamic voltage restorer in electrical distribution system: An overview," *Indonesian Journal of Electrical Engineering and Computer Science*, vol. 17, no. 1, pp. 86–93, 2019.

[2] H. Hafezi and R. Faranda, "Dynamic Voltage Conditioner: A New Concept for Smart Low-Voltage Distribution Systems," *IEEE Transactions on Power Electronics*, vol. 33, no. 9, pp. 7582–7590, 2018.

[3] J. A. K. Mohammed, A. A. Hussein, and S. R. Al-Sakini, "Voltage disturbance mitigation in Iraq's low voltage distribution system," *Indonesian Journal of Electrical Engineering and Computer Science*, vol. 17, no. 1, pp. 47–60, 2019.

[4] A. H. Abed, J. Rahebi, H. Sajir, and A. Farzamnia, "Protection of sensitive loads from voltages fluctuations in Iraqi grids by DVR," 2*017 IEEE 2nd International Conference on Automatic Control and Intelligent Systems (I2CACIS)*, pp. 144–149, 2017.

[5] A. Pakharia and M. Gupta, "Dynamic Voltage Restorer for C Ompensation of Voltage Sag and Swell : a Literature Review," *International Journal of Advances in Engineering & Technology*, vol. 4, no. 1, pp. 347–355, 2012.

[6] D. V. Chinmay and D. V. Chaitanya, "Optimum design of dynamic voltage restorer for voltage sag mitigation in distribution network," *International Journal of Power Electronics and Drive systems (IJPEDS)*, vol. 10, no. 3, pp. 1364-1372, 2019.

[7] D. Danalakshmi, S. Bugata, and J. Kohila, "A control strategy on power quality improvement in consumer side using custom power device," *Indonesian Journal of Electrical Engineering and Computer Science*, vol. 15, no. 1, pp. 80–87, 2019.

[8] P. T. Cheng, J. M. Chen, and C. L. Ni, "Design of a state-feedback controller for series voltage-sag compensators," *IEEE Transactions on Industry Applications*, vol. 45, no. 1, pp. 260–267, 2009.

[9] P. S. Babu and N. Kamaraj, "Performance investigation of dynamic voltage restorer using PI and fuzzy controller," *International Conference on Power, Energy and Control (ICPEC)*, pp. 467–472, 2013.

[10] S. Biricik, H. Komurcugil, and M. Basu, "Sliding mode control strategy for three-phase DVR employing twelve-switch voltage source converter," *IECON 2015-41st Annual Conference of the IEEE Industrial Electronics Society*, pp. 921–926, 2015.

[11] V. F. Pires, M. Guerreiro, and J. F. Silva, "Dynamic voltage restorer using a multilevel converter with a novel cell structure," 2*011 IEEE EUROCON-International Conference on Computer as a Tool*, pp. 1-4, 2011.

[12] S. Biricik and H. Komurcugil, "Optimized Sliding Mode Control to Maximize Existence Region for Single-Phase Dynamic Voltage Restorers," *IEEE Transactions on Industrial Informatics*, vol. 12, no. 4, pp. 1486–1497, 2016.

[13] K. Jeyaraj, D. Durairaj, and A. I. S. Velusamy, "Development and performance analysis of PSO-optimized sliding mode controller–based dynamic voltage restorer for power quality enhancement," *International Transactions on Electrical Energy Systems*, vol. 30, no. 3, pp. 1–14, 2019.

[14] N. Kassarwani, J. Ohri, and A. Singh, "Performance analysis of dynamic voltage restorer using modified sliding mode control," *International Journal of Electronics Letters*, vol. 7, no. 1, pp. 25–39, 2019.

[15] S. A. Al-Samarraie and M. Hussein Mishary Me, "A Chattering Free Sliding Mode Observer with Application to DC Motor Speed Control," *Third Scientific Conference of Electrical Engineering (SCEE)*, pp. 259–264, 2018.

[16] Z. Rayeen, S. Tiwari, and O. Hanif, "Fractional Order PID controller for tuning Interleaved Cuk Converter," *International Conference on Electrical, Engineering (UPCON)*, pp. 1–6, 2019.

[17] K. J. A. and T. Hagglund, "PID controllers, Theory, design and tuning," *Research Triangle Park, NC Instrument Society of America*, vol. 2. 1995.

[18] H. O. Bansal, R. Sharma, and P. R. Shreeraman, "PID Controller Tuning Techniques: A Review," *Journal of control engineering and technology*, vol. 2, no. 4, pp. 168–176, 2012.

[19] A. Basu, S. Mohanty, and R. Sharma, "Designing of the PID and FOPID controllers using conventional tuning techniques," *2016 International conference on inventive computation technologies (ICICT)*, vol. 2, no. 1, 2016.

[20] J. Han and C. Moraga, "The influence of the sigmoid function parameters on the speed of backpropagation learning," *International Workshop on Artificial Neural Networks. Springer, Berlin, Heidelberg*, pp. 195–201, 1995.

[21] A. M. Saeed, S. H. E. Abdel Aleem, A. M. Ibrahim, M. E. Balci, and E. E. A. El-Zahab, "Power conditioning using dynamic voltage restorers under different voltage sag types," j*ournal of advanced research*, vol. 7, no. 1, pp. 95–103, 2016.

[22] "IEEE guide for voltage sag indices" *IEEE Std* 1564, pp. 1–55, 2014.

[23] A. I. Omar, S. H. E. Abdel Aleem, E. E. A. El-Zahab, M. Algablawy, and Z. M. Ali, "An improved approach for robust control of dynamic voltage restorer and power quality enhancement using grasshopper optimization algorithm," *ISA transactions*, vol. 95, pp. 110–129, 2019.

[24] F II, I. "IEEE recommended practices and requirements for harmonic control in electrical power systems," *New York, NY 10017, USA*, 1992.